REPORT

Catalytic conversion of mixed polyolefins under mild atmospheric pressure

Binzhi Zhao,[1] Hui Tan,[1] Jie Yang,[4] Xiaohui Zhang,[1] Zidi Yu,[2] Hanli Sun,[2] Jialiang Wei,[1] Xinyi Zhao,[1] Yufeng Zhang,[1] Lili Chen,[1] Dali Yang,[3] Jin Deng,[4] Yao Fu,[4] Zheng Huang,[5] and Ning Jiao[1,5,*]

*Correspondence: jiaoning@pku.edu.cn

Received: August 16, 2023; Accepted: January 31, 2024; Published Online: February 3, 2024; https://doi.org/10.1016/j.xinn.2024.100586

GRAPHICAL ABSTRACT

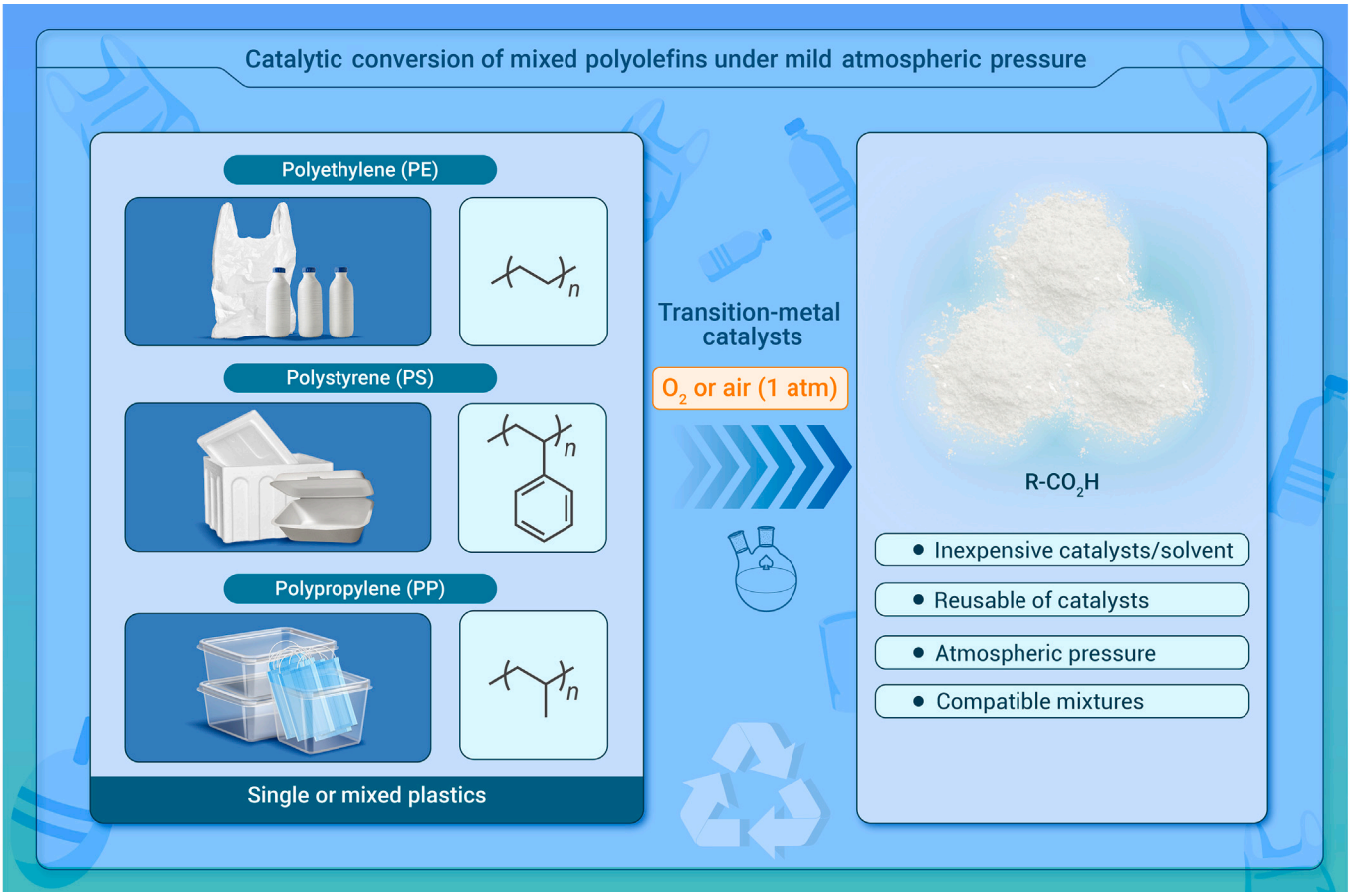

PUBLIC SUMMARY

- Under atmospheric pressure and mild conditions with O_2 or air as the oxidant.
- Compatible with HDPE, LDPE, PS, PP, and mixed polyolefins.
- Economical and recoverable metal catalyst.

REPORT

Catalytic conversion of mixed polyolefins under mild atmospheric pressure

Binzhi Zhao,[1] Hui Tan,[1] Jie Yang,[4] Xiaohui Zhang,[1] Zidi Yu,[2] Hanli Sun,[2] Jialiang Wei,[1] Xinyi Zhao,[1] Yufeng Zhang,[1] Lili Chen,[1] Dali Yang,[3] Jin Deng,[4] Yao Fu,[4] Zheng Huang,[5] and Ning Jiao[1,5,*]

[1]State Key Laboratory of Natural and Biomimetic Drugs, School of Pharmaceutical Sciences, Peking University, Beijing 100191, China

[2]Beijing National Laboratory for Molecular Sciences, College of Chemistry and Molecular Engineering, Peking University, Beijing 100871, China

[3]The Institute for Advanced Studies, Wuhan University, Wuhan 430072, China

[4]Hefei National Laboratory for Physical Sciences at the Microscale, CAS Key Laboratory of Urban Pollutant Conversion, Anhui Province Key Laboratory of Biomass Clean Energy, iChEM, University of Science and Technology of China, Hefei 230026, China

[5]State Key Laboratory of Organometallic Chemistry, Chinese Academy of Sciences, Shanghai 200032, China

*Correspondence: jiaoning@pku.edu.cn

Received: August 16, 2023; Accepted: January 31, 2024; Published Online: February 3, 2024; https://doi.org/10.1016/j.xinn.2024.100586

Citation: Zhao B., Tan H., Yang J., et al., (2024). Catalytic conversion of mixed polyolefins under mild atmospheric pressure. The Innovation **5(2)**, 100586.

The chemical recycling of polyolefin presents a considerable challenge, especially as upcycling methods struggle with the reality that plastic wastes typically consist of mixtures of polyethylene (PE), polystyrene (PS), and polypropylene (PP). We report a catalytic aerobic oxidative approach for polyolefins upcycling with the corresponding carboxylic acids as the product. This method encompasses three key innovations. First, it operates under atmospheric pressure and mild conditions, using O_2 or air as the oxidant. Second, it is compatible with high-density polyethylene, low-density polyethylene, PS, PP, and their blends. Third, it uses an economical and recoverable metal catalyst. It has been demonstrated that this approach can efficiently degrade mixed wastes of plastic bags, bottles, masks, and foam boxes.

INTRODUCTION

Plastics, renowned for their high performance and cost-effectiveness, are extensively used across various industries including packaging, textiles, medical care, construction, transportation, and electronics, significantly contributing to the advancement of modern society. The global annual production of plastics has now surpassed 360 million tons.[1,2] However, the accumulation of plastic waste has resulted in severe environmental issues. Polyolefins, encompassing polyethylene (PE), polystyrene (PS), and polypropylene (PP), represent nearly two-thirds of the total post-consumer plastic waste (Figure 1A).[1,3] The COVID-19 pandemic has further exacerbated this issue, leading to a surge in the use of disposable polyolefins, such as medical packaging, masks, and gloves.[4] Current disposal methods of these materials, primarily landfill and incineration,[1] pose significant environmental threats.[5] Mechanical recycling,[6–8] the predominant method for plastic recycling, requires sorting to obtain pure polymers, but often leads to a decline in the performance of most plastics. The development of chemical recycling methods[9–13] is seen as a promising and much-needed solution for mitigating polyolefin waste pollution. However, the chemical inertness of aliphatic C-H and C-C bonds, their condensed state, as well as high molecular weight make chemical recycling of polyolefins, especially in an upcycling manner, extremely challenging.[14–28] So far, the practical implementation of chemical upcycling for polyolefins is still in its nascent stages.

PP and PE (high-density polyethylene [HDPE], low-density polyethylene [LDPE], and linear low-density polyethylene [LLDPE]) account for 50% of all plastic waste (Figure 1A).[1] Regrettably, these plastics are generally considered less degradable. Intriguingly, recent developments have led to novel upcycling methods specifically for PE.[29–41] Concurrently, a series of photocatalytic chemical recovery methods for PS have also been developed.[42–50] Despite these advancements, the upcycling of PS under mild non-light conditions, the upcycling of PE under mild conditions,[51] and especially the upcycling of mixed polyolefins, have not yet been accomplished. Recently, Beckham, Stahl, and their colleagues have demonstrated significant chemical oxidation of mixed PE and PS, using the resulting products for further biological funneling treatment (Figure 1B).[52] This research has substantially advanced the field of polyolefin upcycling; however, their approach to the chemical oxidation of mixed plastics still necessitates harsh conditions, such as high temperatures (180°C) and high pressures (80 atm), which may lead to coking and dependence on high-pressure equipment. Therefore, there is considerable scope for the optimization and improvement of the oxidative degradation process for mixed plastics.

The groundbreaking findings discussed above will advance the exploration of a more feasible method for upcycling polyolefins, encompassing the following requirements (Figure 1C): (1) mild reaction temperature; (2) atmospheric pressure to circumvent the constraints of large-volume and high-pressure reaction vessels; (3) neutral solvent with superior solubility to address issues of corrosion, efficiency, and space utilization; (4) cost-effective and/or recyclable catalysts; and (5) compatibility with mixed polyolefins. By adhering to these criteria, this approach holds the potential to overcome the existing challenges in polyolefin upcycling, thereby laying the groundwork for a more sustainable and environmentally benign future.

Inspired by recent advancements in oxidative C-C bond cleavage reactions,[53–60] we report a catalytic aerobic oxidation system, capable of upcycling PE, PS, PP, and their blends under mild conditions and atmospheric pressure (Figure 1D). This system is also compatible with polyvinylchloride (PVC). Importantly, the utilization of a highly soluble neutral solvent and atmospheric pressure addresses the challenges of size and high-pressure limitations in scaling up high-pressure reactors. The implementation of simple air flow at atmospheric pressure effectively enables the upcycling of mixed plastic bags, bottles, masks, and foam boxes, yielding corresponding carboxylic acids. This approach may offer a solution for upcycling of non-sorting plastic wastes.

RESULTS AND DISCUSSION

Following numerous screening attempts, we have identified an economical bimetallic catalytic system, consisting of $CoCl_2 \cdot 6H_2O$ and $MnSO_4 \cdot H_2O$, capable of efficiently degrading HDPE under atmospheric pressure, producing dicarboxylic acids as the product (see supplemental information 4.1). Subsequently, polystyrene was selected as the template substrate to optimize the degradation conditions (Table 1). Remarkably, even under relatively mild conditions and atmospheric pressure, styrofoam (M_n = 69.5 kDa) underwent degradation, resulting in a 75% yield of benzoic acid (Table 1, entry 1). Both the ^{1}H NMR (nuclear magnetic resonance spectroscopy) and GPC (gel permeation chromatography) confirmed the complete degradation of the starting material PS. Given the presence of additives and foaming agents in styrofoam,[61] the efficiency of the present protocol is notably high. The protocol's efficacy can be attributed to the use of *n*-butyl acetate as a solvent with excellent solubility for polystyrene, crucial for facilitating the reaction under normal pressure (Table 1). Additionally, classical solvents used in traditional oxidation reactions such as acetic acid, chlorobenzene, and mixtures, did not enhance the reaction (Table 1, entries 5–7). Most significantly, the present oxidative upcycling procedure operates exceptionally well using air as the sole oxidant under atmospheric pressure (Table 1, entry 15), obviating the need for high-pressure reaction vessels and enabling large-scale, safe polyolefin upcycling.

Interestingly, it was observed that throughout the reaction process, the concentration of manganese ions remained consistently low (Figure 2A, left), whereas the concentration of cobalt ions peaked during the first hour and subsequently decreased to the same level as that of manganese ions. Additionally, the formation of solid precipitates upon the completion of the reaction indicated the potential for catalyst recycling. When these precipitates were used as a metal catalyst with an addition of 6% HBr for the next run, the yield of the target product was only 37% (Table S5). Intriguingly, with each addition of only 1 mol % $CoCl_2 \cdot 6H_2O$ and 6 mol % HBr each time, the recovered catalyst could be

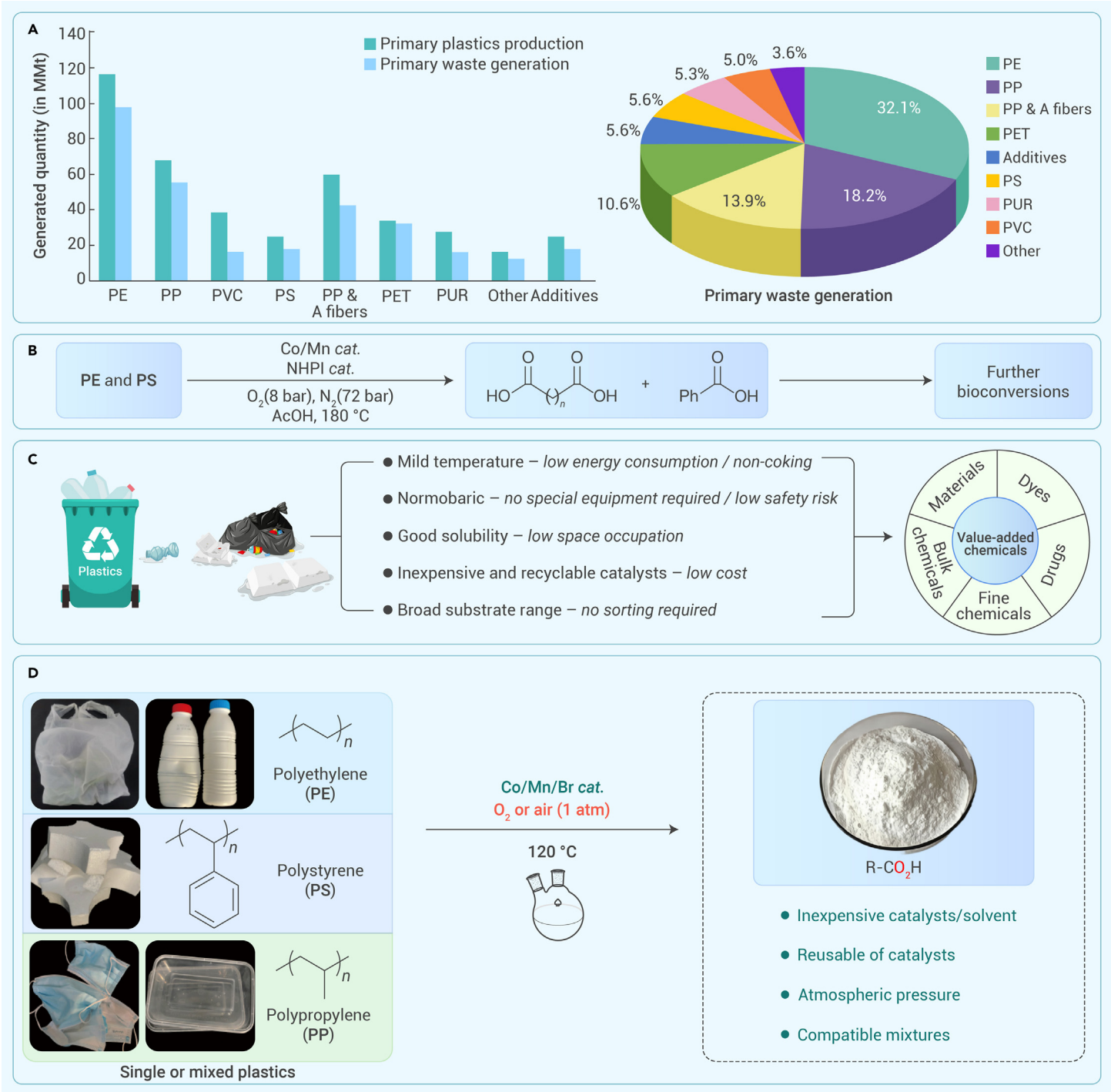

Figure 1. Current situation of plastics and degradation strategies (A) Global primary plastics production and primary waste generation in 2015. (B) The upcycling of mixed polyolefins. (C) The requirements for a practical plastic degradation method. (D) Aerobic oxidative carboxylation with mild conditions.

successfully reused for eight consecutive runs at the same scale as the initial reaction (1.04 g), achieving yields between 50% and 70% (Figure 2A, right). These findings demonstrate the potential for recycling this cost-effective catalyst combination.

To accurately study the upcycling of PE and PP, deuterated solvents were utilized to eliminate background reactions stemming from solvent hydrolysis and oxidation. As depicted in Figure 2B, LDPE (M_n = 29.9 kDa) produced acetic acid, formic acid, and C4-C7 dicarboxylic acids in yields of 5.5%, 9.7%, and 16.2%, respectively. Notably, succinic and glutaric acids constituted 97% of the total dicarboxylic acids. Moreover, HDPE (M_n = 38.7 kDa) produced 5.6% acetic acid, 9.2% formic acid, and C4-C7 dicarboxylic acids at a yield of 23%, with 93% being succinic and glutaric acids. These dicarboxylic acids can be further transformed into value-added compounds.[18,52] The complete degradation of the polymer was confirmed by GPC, with no residual polymer detected. Significantly, CO_2 was observed in the gas phase of the reaction system (Figure S105). Under standard conditions, PP selectively converted into acetic acid and formic acid with yields of 41% and 22%, respectively (Figure 2C), and no residual polymer was detected by GPC after the post-reaction.

Remarkably, using air as the oxidant with a small air pump, 52.3 g of styrofoam was upcycled into benzoic acid with an isolated yield of 59% (Figure 3A). To further validate the utility of this protocol, a mixture of 2.1 g of disposable plastic gloves and droppers (LDPE) was degraded, resulting in a 33% yield of dicarboxylic acids, of which C4-C9 dicarboxylic acids constituted 85% of the total products. Additionally, the system contained 636% acetic acid and 57% formic acid, partially obtained through hydrolysis

Table 1. Optimization of reaction conditions

Entry	Derivation from standard conditions[a]	Yield (mol %)
1	None	75 (66)
2	no $CoCl_2 \cdot 6H_2O$	trace
3	no $MnSO_4 \cdot H_2O$	14
4	no HBr	25
5	AcOH instead of AcO^{n}Bu	0
6	PhCl instead of AcO^{n}Bu	0
7	AcOH: PhCl (1:1) instead of AcO^{n}Bu	0
8	1,4-Dioxane instead of AcO^{n}Bu	0
9	PhCl instead of AcO^{n}Bu, ^{n}PrCHO (20 mol %)	39
10	NaBr instead of HBr	74
11	r.t. instead of 120°C	0
12	[Co]:[Mn] = 1:1 ([Mn] = 1 mol %)	77 (67)
13	M_w = 35 kDa (standard conditions)	71
14	M_p = 15,188 kDa (standard conditions)	76
15[b]	air flow instead of O_2	61

[a]Reaction conditions: Styrofoam (83.0 mg, M_n = 69.5 kDa, 0.8 mmol, based on the repeating styrene unit), $CoCl_2 \cdot 6H_2O$ (3 mol %, based on the repeating styrene unit), $MnSO_4 \cdot H_2O$ (3 mol %), HBr (48% aqueous solution, 6 mol %) in AcO^{n}Bu (2.0 mL) at 120°C under O_2 (balloon) for 36 h. Yields were determined by ^{1}H NMR using 1,1,2,2-tetrachloroethane as internal standard, the isolated yield was indicated in parenthesis. The yield of benzoic acid was based on the single repeat unit (theoretical yield: 100%).
[b]Styrofoam (1.04 g, M_n = 69.5 kDa) under air flow (120 mL/min).

and oxidation of the solvent (see supplemental information 5.3). Only 0.6 g of solid residue (M_n = 0.7 kDa) was recovered post-reaction (Figure 3B). Similarly, 2.1 g of milk bottle (HDPE) was converted into dicarboxylic acids with a 41% yield, including 75% of C4-C9 dicarboxylic acids, alongside the detection of acetic acid and formic acid. In this instance, 0.7 g of solid residue remained (Figure 3B). Intriguingly, 22.0 g of surgical masks (excluding the wire and cotton mask straps) were successfully degraded, yielding acetic acid and formic acid with an 89% conversion rate, while a PP lunch box of the same weight exhibited a conversion rate of 78% (Figure 3C).

Encouraged by the preceding results, the degradation of mixed polyolefins under standard conditions was explored (Figures 3D–3F). A mixture of LDPE, PS, and PP totaling 17.4 g was degraded together, producing benzoic acid at a 72% yield with an overall conversion rate of 86% (Figure 3D). In this instance, besides benzoic acid, only acetic acid and formic acid were prominently detected in the filtrate by ^{1}H NMR. Excitingly, the mixture of HDPE, PP, and PS weighing 24.4 g in total could also be degraded using air as the oxidant with a simple air pump (Figure 3F).

The mixture of PP, PS, LDPE, and PVC, totaling 23.7 g, produced benzoic acid in at a 91% yield and a 26% yield of mixed dicarboxylic acids, of which C4-C9 dicarboxylic acids constituted 94% of the total dicarboxylic acids. The ^{1}H NMR spectrum of the solution indicated the presence of 1,547% acetic acid and 168% formic acid, while the GPC traces of the reaction solution revealed M_n of 7.7 kDa (Figure 3E). These results demonstrate that the presence of PVC does not adversely impact the efficiency of the current catalytic protocol for degrading mixed polyolefins. Given the presence of additives and forming agents in these plastic materials, the efficiency and conversion rate of this protocol are considered quite satisfactory.

Subsequently, a preliminary characterization of the recovered metal catalyst was performed. In the X-ray diffraction (XRD) pattern of the recovered metal catalyst (Figure 4A), a series of distinct diffraction peaks were observed, which could be indexed to $MnSO_4 \cdot 4H_2O$ (JCPDS 33–0906) and $CaSO_4 \cdot 0.62H_2O$ (JCPDS 47–0964). (Since real plastic [Styrofoam] was used in this experiment, then it would contain some additives such as calcium carbonate.[61] The calcium element contained in the catalyst obtained by recycling should come from the plastic additives.) The content of cobalt in the recovered catalyst determined by ICP-MS was as high as 11.5 wt %, although no signal of Co species was observed in the XRD pattern. These results suggest that the Co species in the recovered metal catalyst is in an amorphous state. The composition and chemical nature of the recovered metal catalyst were analyzed by X-ray photoelectron spectroscopy (XPS), as shown in Figures 4B, 4C, and S97. The peaks with bonding energies at approximately 782.1, 642.1, 532.1, and 285.1 eV correspond to Co 2p3/2, Mn 2p3/2, C 1s, and O 1s, respectively (Figure S97). In the high-resolution XPS spectra, the Mn 2p3/2 peak was deconvoluted into three peaks (641.2 eV, 642.7 eV, and 646.4 eV), attributed to Mn^{2+}, Mn^{3+}, and a satellite peak, respectively.[62,63] The Co 2p3/2 peaks, centered at 781.0, 783.0, and 786.3 eV, were ascribed to Co^{2+}, Co^{3+}, and a satellite peak, respectively.[63,64] The hexagonal peak signals in the electron paramagnetic resonance (EPR) experiments of the aqueous solution of the recovered metal catalyst were attributed to Mn^{2+} (Figure 4D).[65] The electronic and coordination structures of cobalt atoms were analyzed using X-ray absorption fine structure (XAFS) techniques. The X-ray absorption near edge structure (XANES) analysis indicated that the energy absorption threshold of cobalt lay between the $Co(OH)_2$ and Co_2O_3 standards, suggesting that the majority of cobalt atoms in the catalyst were positively charged, possibly in a mixed valence state (Figure 4E). The Fourier transformed (FT) k^2-weighted extended X-ray absorption fine structure (EXAFS) spectra of the recovered metal catalyst exhibited a prominent peak at approximately 1.6 Å (unphased corrected), falling between the Co-O scattering peaks of $Co(OH)_2$ and Co_2O_3 (Figure 4F), suggesting an amorphous state of cobalt in the recovered metal catalyst with Co-O coordination. The EXAFS fitting results (Figures S98, S99, and Table S18) further revealed an average Co-O bond distance of 2.08 Å in the recovered catalyst. Additionally, a minor secondary scattering feature was well-fitted to a Co-Co scattering path, indicating the presence of a very small amount of Co(0) nanoparticles. No Co-Cl scattering path was detected.

Figures 5A and 5B, respectively, illustrate the time courses of benzoic acid formation and the overall molecular weight (M_n) of the reaction system during the degradation of PS. These findings reveal that the polymer degradation was exceptionally rapid in the first hour (M_n decreasing from 69.5 kDa to 6.7 kDa), subsequently slowing down (Figure 5B). Notably, the generation of target products does not occur in synchrony with the degradation of polymer chains (Figures 5A and 5B). As the reaction progresses, the molecular weight of the system gradually shifts from higher to lower values, with a corresponding decrease in dispersity (Figure 5C).

To elucidate the role of individual components of the Co/Mn/Br ternary catalyst in this reaction, a series of controlled experiments were conducted (see supplemental information 5.1). Based on the results in supplemental information 5.1.3, it is clear that the cobalt catalyst plays a pivotal role in the reaction, with the manganese and bromine catalysts acting as auxiliary catalysts. Cobalt catalyzes the conversion of polyolefins into corresponding carboxylic acids. While manganese and bromine catalysts can only cleave the polymer chain and not convert them into carboxylic acids, their addition enhances the catalytic activity of cobalt, leading to an increased yield of carboxylic acids. According to the results in supplemental information 5.1.4, HBr significantly enhances the dissolution of metal ions (Co/Mn) in the solution, highlighting an additional role of bromine in the reaction. We propose that the combination of catalysts drives a catalytic process akin to the reported Co/Mn/Br catalysis under high-pressure conditions.[14,66,67]

The screening results presented in Table 1 underscore the essential role of *n*-butyl acetate as a solvent in the present mild degradation reaction. To elucidate the critical role of *n*-butyl acetate, several supplementary experiments (see supplemental information 5.4) were conducted, investigating the potential reaction of the solvent under standard conditions without polyolefins. Intriguingly, *n*-butanol, *n*-butyraldehyde, and *n*-butyric acid were detected by gas chromatography-mass spectrometry (GC-MS) (Figure 5D). As indicated in supplemental information 5.4, the significance of *n*-butyl acetate as a solvent in this discovery encompasses two critical functions: (1) it demonstrates excellent solubility for polyolefins, ensuring effective dissolution of these polyolefins; and (2) the solvent facilitates the continuous generation of key components such as *n*-butanol and subsequent *n*-butyraldehyde. We hypothesize that *n*-butyraldehyde may undergo oxidation into peroxide species, further enhancing the current oxidative degradation,[68,69] which was corroborated by a control reaction with the addition of extra *n*-butyraldehyde (Table 1, entry 9; supplemental information 5.4.2, entry 3). To date, the mechanism

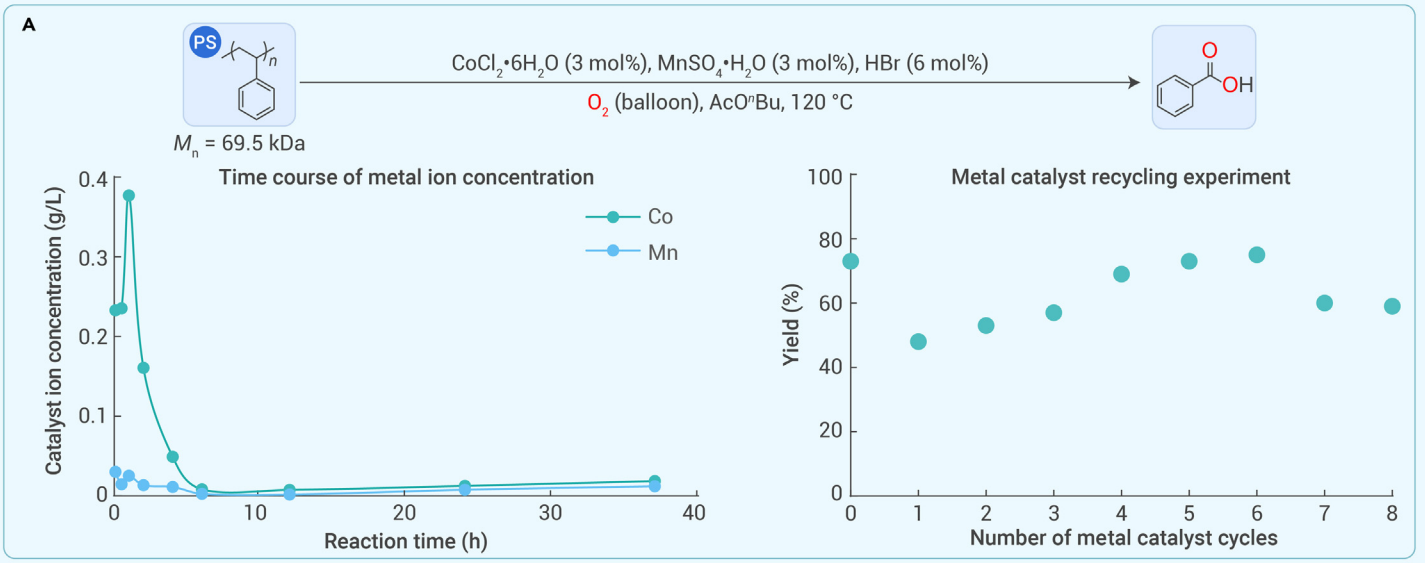

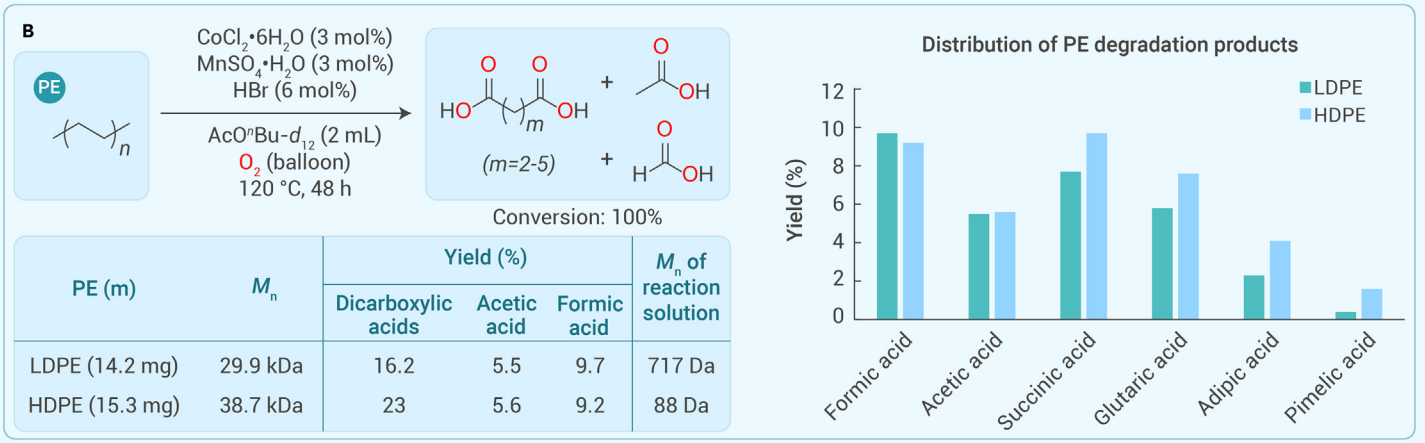

PE (m)	M_n	Yield (%)			M_n of reaction solution
		Dicarboxylic acids	Acetic acid	Formic acid	
LDPE (14.2 mg)	29.9 kDa	16.2	5.5	9.7	717 Da
HDPE (15.3 mg)	38.7 kDa	23	5.6	9.2	88 Da

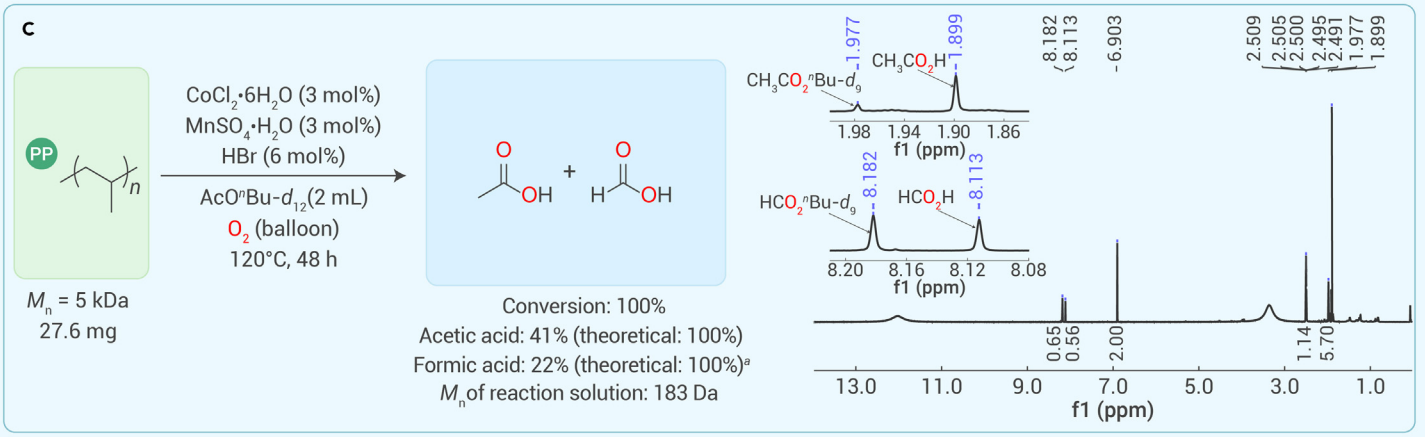

Figure 2. Degradation of polyolefins (A) (Left) Time course of metal ions concentration monitored by ICP-MS in PS degradation. (Right) Metal catalyst recycling experiment in PS degradation (styrofoam, 1.04 g in each recycling run, M_n = 69.5 kDa). (B) Degradation of PE to dicarboxylic acids. (C) Degradation of PP to acetic acid and formic acid. [a]The yield of acetic acid was based on the repeating $CHCH_3$ unit of PP (theoretical yield: 100%), and the yield of formic acid was based on the corresponding repeating CH_2 unit of PP (theoretical yield: 100%). The yields of both PS and PE degradation products were determined based on a single replicate unit (theoretical yield: 100%). Polymer feedstocks and catalysts were quantified by the corresponding repeating monomer unit.

of this mild protocol remains incompletely understood, with more comprehensive mechanistic studies under way.

CONCLUSION

In summary, a general method has been developed for the upcycling of polyolefins under atmospheric pressure, utilizing O_2 or air as the oxidant. This approach has been extended to effectively degrade a mixture of waste plastic bags, bottles, masks, and foam boxes. Considering the recent advancements in microbial metabolic engineering by Beckham, Stahl, and their colleagues, these mixtures of organic acids can be further converted into more singular and valuable organic compounds through biological funneling treatment. We anticipate that the employment of cost-effective catalysts, alongside recovered metal catalysts and the safe operating conditions, will significantly enhance the industrial recycling of waste plastics.

MATERIALS AND METHODS

See supplemental information for details.

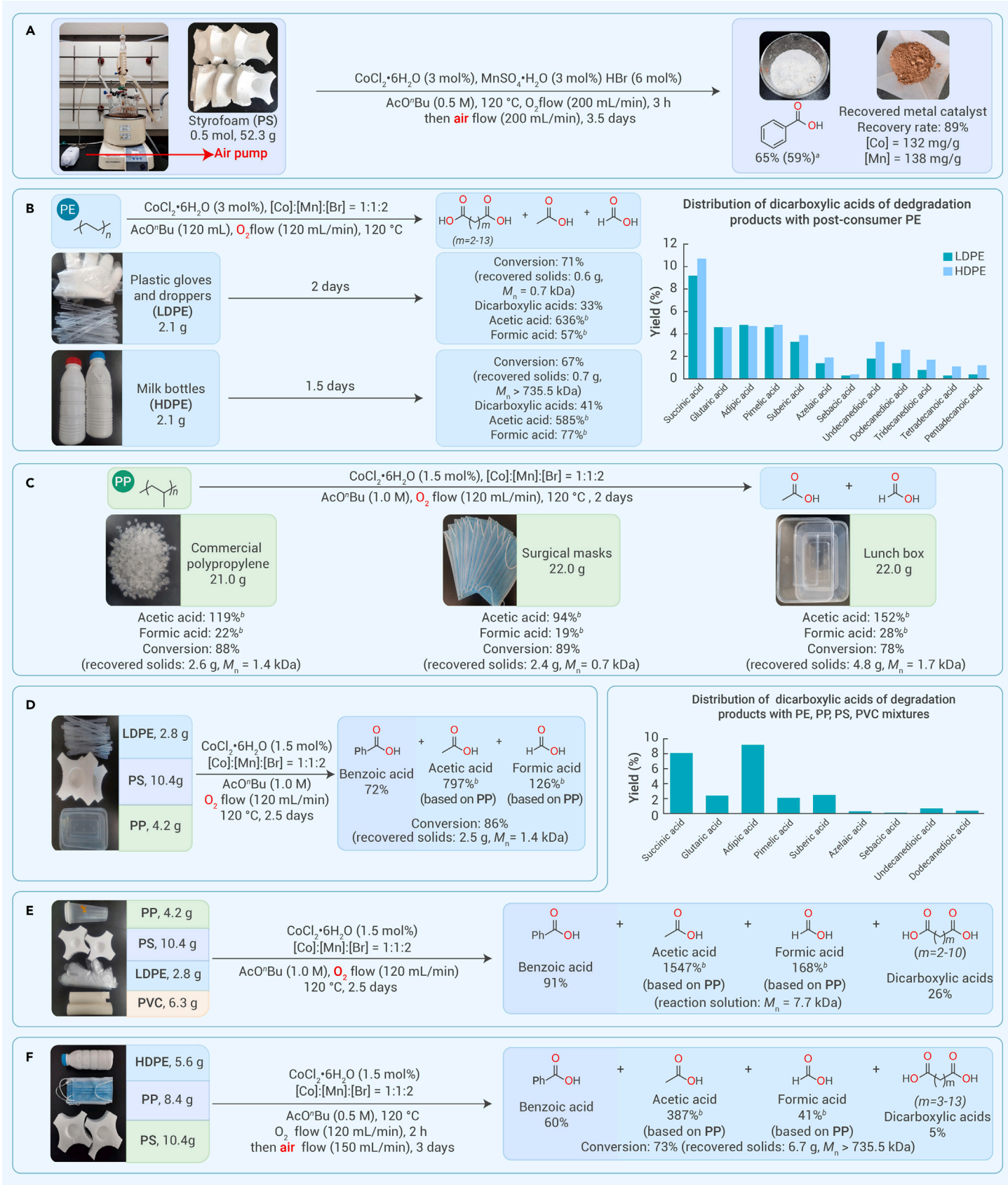

Figure 3. Practical application (gram scale) (A) Degradation of styrofoam (PS) under air atmosphere. (B) Degradation of disposable plastic gloves and droppers (LDPE) and milk bottles (HDPE). (C) Degradation of PP (commercial polypropylene, surgical masks and disposable lunch boxes). (D) Degradation of mixed polyolefins (LDPE, PS, and PP). (E) Degradation of mixed polyolefins (PS, PP, LDPE, and PVC). (F) Degradation of mixed polyolefins (HDPE, PP, and PS) under air atmosphere. [a]Isolated yield. [b]Since some solvents can also produce acetic acid and formic acid, the yield of acetic acid and formic acid could not be accurately calculated, and the total amount of acetic acid and formic acid at the end of the reaction was determined by ^{1}H NMR. The yield calculations were the same as in Figure 2.

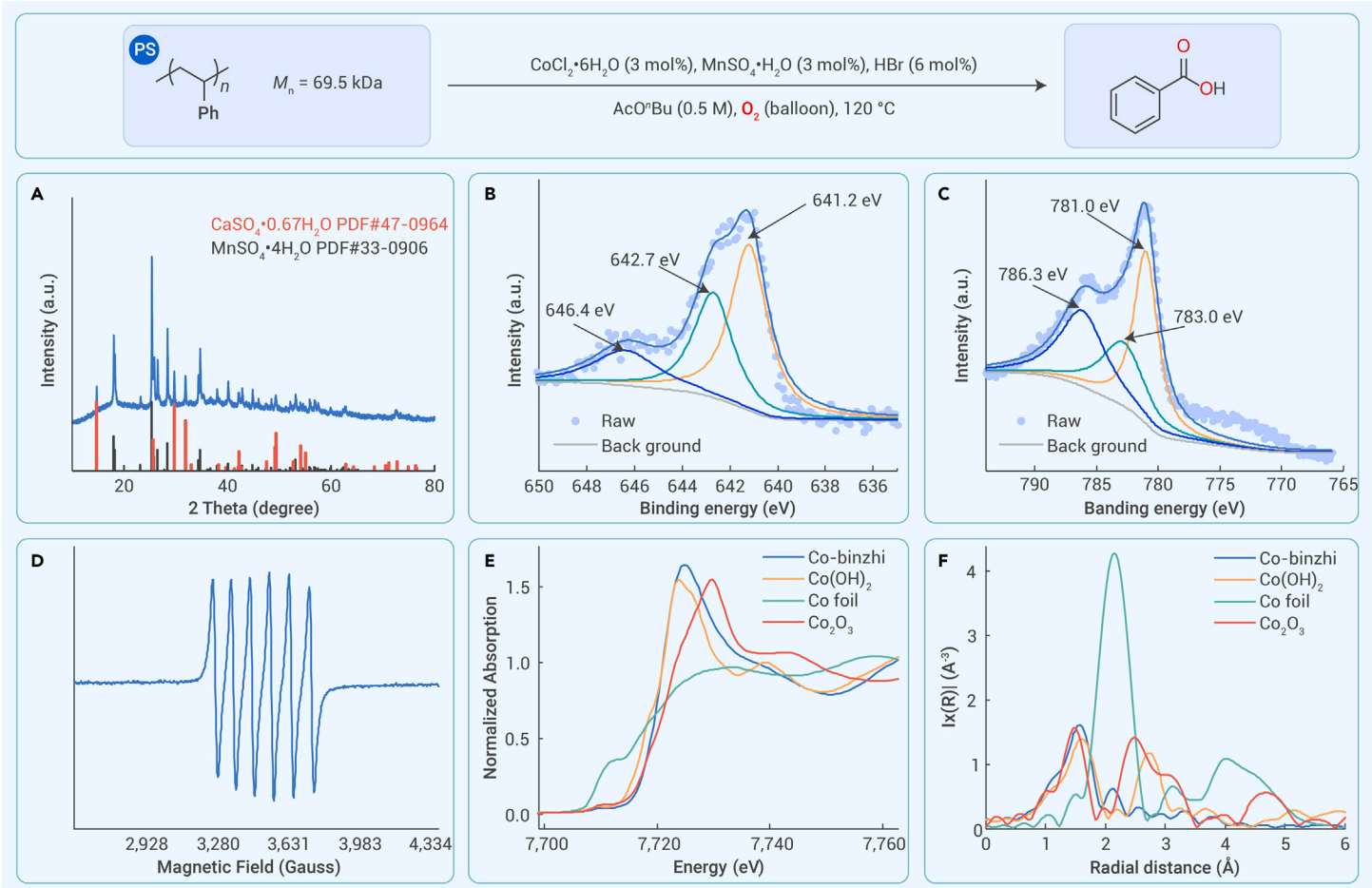

Figure 4. Recovered metal catalyst characterization (A) Survey scan XRD patterns of the recovered metal catalyst of PS degradation. (B) XPS spectra of Mn 2p3/2 for the recovered metal catalyst of PS degradation. (C) XPS spectra of Co 2p3/2 for the recovered metal catalyst of PS degradation. (D) EPR spectra (X band, 9.8 GHz) of the aqueous solution of the recovered metal catalyst at room temperature. (E) XANES spectrum of the recovered metal catalyst with relevant standards at the Co K-edge. (F) FT-EXAFS spectrum of of the recovered metal catalyst with relevant standards.

REFERENCES

1. Geyer, R., Jambeck, J.R., and Law, K.L. (2017). Production, use, and fate of all plastics ever made. Sci. Adv. ***3***(7): e1700782. https://doi.org/10.1126/sciadv.1700782.
2. Nicholson, S.R., Rorrer, N.A., Carpenter, A.C., et al. (2021). Manufacturing energy and greenhouse gas emissions associated with plastics consumption. Joule ***5***(3): 673–686. https://doi.org/10.1016/j.joule.2020.12.027.
3. Chamas, A., Moon, H., Zheng, J., et al. (2020). Degradation rates of plastics in the environment. ACS Sustain. Chem. Eng. ***8***(9): 3494–3511. https://doi.org/10.1021/acssuschemeng.9b06635.
4. Patrício Silva, A.L., Prata, J.C., Walker, T.R., et al. (2021). Increased plastic pollution due to COVID-19 pandemic: challenges and recommendations. Chem. Eng. J. ***405***: 126683. https://doi.org/10.1016/j.cej.2020.126683.
5. MacLeod, M., Arp, H.P.H., Tekman, M.B., et al. (2021). The global threat from plastic pollution. Science ***373***(6550): 61–65. https://doi.org/10.1126/science.abg5433.
6. Moens, E.K.C., De Smit, K., Marien, Y.W., et al. (2020). Progress in reaction mechanisms and reactor technologies for thermochemical recycling of poly(methyl methacrylate). Polymers ***12***(8): 1667. https://doi.org/10.3390/polym12081667.
7. De Smit, K., Wieme, T., Marien, Y.W., et al. (2022). Multi-scale reactive extrusion modelling approaches to design polymer synthesis, modification and mechanical recycling. React. Chem. Eng. ***7***(2): 245–263. https://doi.org/10.1039/D1RE00556A.
8. Ceretti, D.V.A., Edeleva, M., Cardon, L., et al. (2023). Molecular pathways for polymer degradation during conventional processing, additive manufacturing, and mechanical recycling. Molecules ***28***(5): 2344. https://doi.org/10.3390/molecules28052344.
9. Ellis, L.D., Rorrer, N.A., Sullivan, K.P., et al. (2021). Chemical and biological catalysis for plastics recycling and upcycling. Nat. Catal. ***4***(7): 539–556. https://doi.org/10.1038/s41929-021-00648-4.
10. Korley, L.T.J., Epps, T.H., Helms, B.A., et al. (2021). Toward polymer upcycling—adding value and tackling circularity. Science ***373***(6550): 66–69. https://doi.org/10.1126/science.abg4503.
11. Kosloski-Oh, S.C., Wood, Z.A., Manjarrez, Y., et al. (2021). Catalytic methods for chemical recycling or upcycling of commercial polymers. Mater. Horiz. ***8***(4): 1084–1129. https://doi.org/10.1039/D0MH01286F.
12. Jehanno, C., Alty, J.W., Roosen, M., et al. (2022). Critical advances and future opportunities in upcycling commodity polymers. Nature ***603***(7903): 803–814. https://doi.org/10.1038/s41586-021-04350-0.
13. Zhang, M.-Q., Wang, M., Sun, B., et al. (2022). Catalytic strategies for upvaluing plastic wastes. Chem ***8***(11): 2912–2923. https://doi.org/10.1016/j.chempr.2022.08.004.
14. Partenheimer, W. (2003). Valuable oxygenates by aerobic oxidation of polymers using metal/bromide homogeneous catalysts. Catal. Today ***81***(2): 117–135. https://doi.org/10.1016/S0920-5861(03)00124-X.
15. Jing, Y., Wang, Y., Furukawa, S., et al. (2021). Towards the circular economy: converting aromatic plastic waste back to arenes over a Ru/Nb_2O_5 catalyst. Angew. Chem. Int. Ed. ***60***(10): 5527–5535. https://doi.org/10.1002/anie.202011063.
16. Pifer, A. and Sen, A. (1998). Chemical recycling of plastics to useful organic compounds by oxidative degradation. Angew. Chem. Int. Ed. ***37***(23): 3306–3308. https://doi.org/10.1002/(SICI)1521-3773(19981217)37:23<3306::AID-ANIE3306>3.0.CO;2-B.
17. Bäckström, E., Odelius, K., and Hakkarainen, M. (2017). Trash to treasure: microwave-assisted conversion of polyethylene to functional chemicals. Ind. Eng. Chem. Res. ***56***(50): 14814–14821. https://doi.org/10.1021/acs.iecr.7b04091.
18. Bäckström, E., Odelius, K., and Hakkarainen, M. (2019). Designed from recycled: turning polyethylene waste to covalently attached polylactide plasticizers. ACS Sustain. Chem. Eng. ***7***(12): 11004–11013. https://doi.org/10.1021/acssuschemeng.9b02092.
19. Xu, Z., Munyaneza, N.E., Zhang, Q., et al. (2023). Chemical upcycling of polyethylene, polypropylene, and mixtures to high-value surfactants. Science ***381***(6658): 666–671. https://doi.org/10.1126/science.adh0993.
20. Anuar Sharuddin, S.D., Abnisa, F., Wan Daud, W.M.A., et al. (2016). A review on pyrolysis of plastic wastes. Energy Convers. Manag. ***115***: 308–326. https://doi.org/10.1016/j.enconman.2016.02.037.
21. Al-Salem, S.M., Antelava, A., Constantinou, A., et al. (2017). A review on thermal and catalytic pyrolysis of plastic solid waste (PSW). J. Environ. Manag. ***197***: 177–198. https://doi.org/10.1016/j.jenvman.2017.03.084.
22. Munir, D., Irfan, M.F., and Usman, M.R. (2018). Hydrocracking of virgin and waste plastics: A detailed review. Renew. Sustain. Energy Rev. ***90***: 490–515. https://doi.org/10.1016/j.rser.2018.03.034.

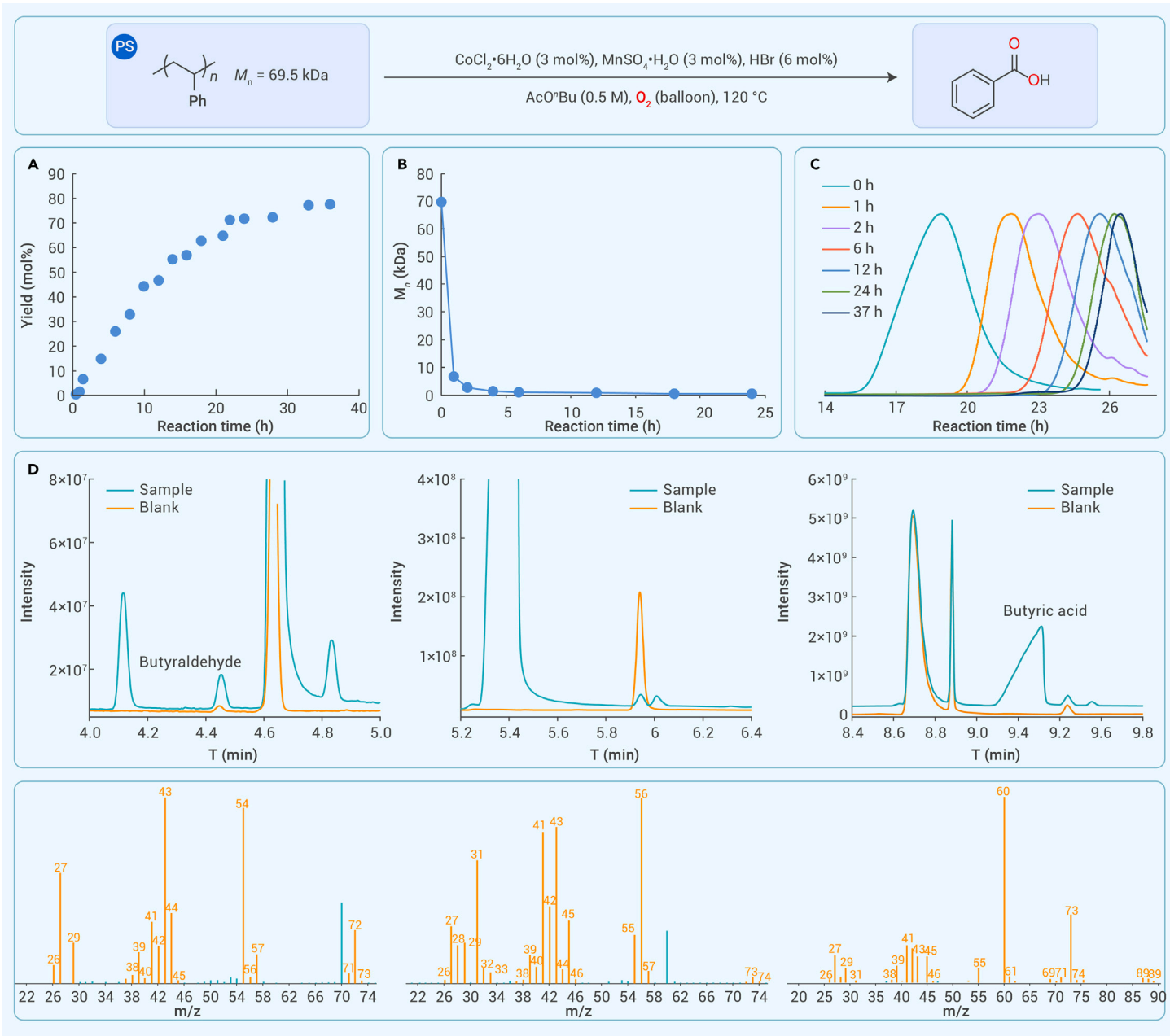

Figure 5. Reaction process investigation (A) Time course of benzoic acid in PS degradation reaction. (B) Overall molecular weight (M_n) of the reaction system during PS degradation. (C) GPC traces of PS degradation reaction. (D) Key products of pure *n*-butyl acetate under standard conditions (without substrate).

23. Liu, S., Kots, P.A., Vance, B.C., et al. (2021). Plastic waste to fuels by hydrocracking at mild conditions. Sci. Adv. ***7***(17): eabf8283. https://doi.org/10.1126/sciadv.abf8283.
24. Hackler, R.A., Lamb, J.V., Peczak, I.L., et al. (2022). Effect of macro- and microstructures on catalytic hydrogenolysis of polyolefins. Macromolecules ***55***(15): 6801–6810. https://doi.org/10.1021/acs.macromol.2c00805.
25. Chen, S., Tennakoon, A., You, K.-E., et al. (2023). Ultrasmall amorphous zirconia nanoparticles catalyse polyolefin hydrogenolysis. Nat. Catal. ***6***(2): 161–173. https://doi.org/10.1038/s41929-023-00910-x.
26. Lee, W.-T., Bobbink, F.D., van Muyden, A.P., et al. (2021). Catalytic hydrocracking of synthetic polymers into grid-compatible gas streams. Cell Rep. Phys. Sci. ***2***(2): 100332. https://doi.org/10.1016/j.xcrp.2021.100332.
27. Wu, X., Tennakoon, A., Yappert, R., et al. (2022). Size-controlled nanopticles embedded in a mesoporous architecture leading to efficient and selective hydrogenolysis of polyolefins. J. Am. Chem. Soc. ***144***(12): 5323–5334. https://doi.org/10.1021/jacs.1c11694.
28. Zichittella, G., Ebrahim, A.M., Zhu, J., et al. (2022). Hydrogenolysis of polyethylene and polypropylene into propane over cobalt-based catalysts. JACS Au ***2***(10): 2259–2268. https://doi.org/10.1021/jacsau.2c00402.
29. Tennakoon, A., Wu, X., Paterson, A.L., et al. (2020). Catalytic upcycling of high-density polyethylene via a processive mechanism. Nat. Catal. ***3***(11): 893–901. https://doi.org/10.1038/s41929-020-00519-4.
30. Wang, K., Jia, R., Cheng, P., et al. (2023). Highly selective catalytic oxi-upcycling of polyethylene to aliphatic dicarboxylic acid under a mild hydrogen-free process. Angew. Chem. Int. Ed. ***62***(29): e202301340. https://doi.org/10.1002/anie.202301340.
31. Jia, X., Qin, C., Friedberger, T., et al. (2016). Efficient and selective degradation of polyethylenes into liquid fuels and waxes under mild conditions. Sci. Adv. ***2***(6): e1501591. https://doi.org/10.1126/sciadv.1501591.
32. Ellis, L.D., Orski, S.V., Kenlaw, G.A., et al. (2021). Tandem heterogeneous catalysis for polyethylene depolymerization via an olefin-intermediate process. ACS Sustain. Chem. Eng. ***9***(2): 623–628. https://doi.org/10.1021/acssuschemeng.0c07612.
33. Zhang, F., Zeng, M., Yappert, R.D., et al. (2020). Polyethylene upcycling to long-chain alkylaromatics by tandem hydrogenolysis/aromatization. Science ***370***(6515): 437–441. https://doi.org/10.1126/science.abc5441.
34. Li, H., Wu, J., Jiang, Z., et al. (2023). Hydroformylation of pyrolysis oils to aldehydes andalcohols from polyolefin waste. Science ***381***(6658): 660–666. https://doi.org/10.1126/science.adh1853.
35. Kanbur, U., Zang, G., Paterson, A.L., et al. (2021). Catalytic carbon-carbon bond cleavage and carbon-element bond formation give new life for polyolefins as biodegradable surfactants. Chem ***7***(5): 1347–1362. https://doi.org/10.1016/j.chempr.2021.03.007.
36. Fazekas, T.J., Alty, J.W., Neidhart, E.K., et al. (2022). Diversification of aliphatic C–H bonds in small molecules and polyolefins through radical chain transfer. Science ***375***(6580): 545–550. https://doi.org/10.1126/science.abh4308.

37. Conk, R.J., Hanna, S., Shi, J.X., et al. (2022). Catalytic deconstruction of waste polyethylene with ethylene to form propylene. Science ***377***(6614): 1561–1566. https://doi.org/10.1126/science.add1088.
38. Wang, N.M., Strong, G., DaSilva, V., et al. (2022). Chemical recycling of polyethylene by tandem catalytic conversion to propylene. J. Am. Chem. Soc. ***144***(40): 18526–18531. https://doi.org/10.1021/jacs.2c07781.
39. Jie, X., Li, W., Slocombe, D., et al. (2020). Microwave-initiated catalytic deconstruction of plastic waste into hydrogen and high-value carbons. Nat. Catal. ***3***(11): 902–912. https://doi.org/10.1038/s41929-020-00518-5.
40. Jiao, X., Zheng, K., Chen, Q., et al. (2020). Photocatalytic conversion of waste plastics into C_2 fuels under simulated natural environment conditions. Angew. Chem. Int. Ed. ***59***(36): 15497–15501. https://doi.org/10.1002/anie.201915766.
41. Rabot, C., Chen, Y., Bijlani, S., et al. (2023). Conversion rate of polyethylenes into fungal secondary metabolites. Angew. Chem. Int. Ed. ***62***(4): e202214609. https://doi.org/10.1002/anie.202214609.
42. Oh, S. and Stache, E.E. (2022). Chemical upcycling of commercial polystyrene via catalyst-controlled photooxidation. J. Am. Chem. Soc. ***144***(13): 5745–5749. https://doi.org/10.1021/jacs.2c01411.
43. Huang, Z., Shanmugam, M., Liu, Z., et al. (2022). Chemical recycling of polystyrene to valuable chemicals via selective acid-catalyzed aerobic oxidation under visible light. J. Am. Chem. Soc. ***144***(14): 6532–6542. https://doi.org/10.1021/jacs.2c01410.
44. Li, T., Vijeta, A., Casadevall, C., et al. (2022). Bridging plastic recycling and organic catalysis: photocatalytic deconstruction of polystyrene via a C–H oxidation pathway. ACS Catal. ***12***(14): 8155–8163. https://doi.org/10.1021/acscatal.2c02292.
45. Qin, Y., Zhang, T., Ching, H.V., et al. (2022). Integrated strategy for the synthesis of aromatic building blocks via upcycling of real-life plastic wastes. Chem ***8***(9): 2472–2484. https://doi.org/10.1016/j.chempr.2022.06.002.
46. Cao, R., Zhang, M.-Q., Hu, C., et al. (2022). Catalytic oxidation of polystyrene to aromatic oxygenates over a graphitic carbon nitride catalyst. Nat. Commun. ***13***(1): 4809. https://doi.org/10.1038/s41467-022-32510-x.
47. Zhang, G., Zhang, Z., and Zeng, R. (2021). Photoinduced $FeCl_3$-catalyzed alkyl aromatics oxidation toward degradation of polystyrene at room temperature. Chin. J. Chem. ***39***(12): 3225–3230. https://doi.org/10.1002/cjoc.202100420.
48. Wang, M., Wen, J., Huang, Y., et al. (2021). Selective degradation of styrene-related plastics catalyzed by iron under visible light. ChemSusChem ***14***(22): 5049–5056. https://doi.org/10.1002/cssc.202101762.
49. Meng, J., Zhou, Y., Li, D., et al. (2023). Degradation of plastic wastes to commercial chemicals and monomers under visible light. Sci. Bull. ***68***(14): 1522–1530. https://doi.org/10.1016/j.scib.2023.06.024.
50. Urgoitia, G., Herrero, M.T., and SanMartin, R. (2022). Metal-catalyzed, photo-assisted selective transformation of tertiary alkylbenzenes and polystyrenes into carbonyl compounds. ChemSusChem ***15***(17): e202200940. https://doi.org/10.1002/cssc.202200940.
51. Zhang, W., Kim, S., Wahl, L., et al. (2023). Low-temperature upcycling of polyolefins into liquid alkanes via tandem cracking-alkylation. Science ***379***(6634): 807–811. https://doi.org/10.1126/science.ade7485.
52. Sullivan, K.P., Werner, A.Z., Ramirez, K.J., et al. (2022). Mixed plastics waste valorization through tandem chemical oxidation and biological funneling. Science ***378***(6616): 207–211. https://doi.org/10.1126/science.abo4626.
53. Qiu, X., Sang, Y., Wu, H., et al. (2021). Cleaving arene rings for acyclic alkenylnitrile synthesis. Nature ***597***(7874): 64–69. https://doi.org/10.1038/s41586-021-03801-y.
54. Liu, M., Zhang, Z., Yan, J., et al. (2020). Aerobic oxidative cleavage and esterification of C(OH)–C bonds. Chem ***6***(12): 3288–3296. https://doi.org/10.1016/j.chempr.2020.09.006.
55. Smaligo, A.J., Swain, M., Quintana, J.C., et al. (2019). Hydrodealkenylative $C(sp^3)$–$C(sp^2)$ bond fragmentation. Science ***364***(6441): 681–685. https://doi.org/10.1126/science.aaw4212.
56. Roque, J.B., Kuroda, Y., Göttemann, L.T., et al. (2018). Deconstructive fluorination of cyclic amines by carbon-carbon cleavage. Science ***361***(6398): 171–174. https://doi.org/10.1126/science.aat6365.
57. Reisenbauer, J.C., Green, O., Franchino, A., et al. (2022). Late-stage diversification of indole skeletons through nitrogen atom insertion. Science ***377***(6610): 1104–1109. https://doi.org/10.1126/science.add1383.
58. Xu, Y., Qi, X., Zheng, P., et al. (2019). Deacylative transformations of ketones via aromatization-promoted C–C bond activation. Nature ***567***(7748): 373–378. https://doi.org/10.1038/s41586-019-0926-8.
59. Woo, J., Christian, A.H., Burgess, S.A., et al. (2022). Scaffold hopping by net photochemical carbon deletion of azaarenes. Science ***376***(6592): 527–532. https://doi.org/10.1126/science.abo4282.
60. Rahimi, A., Ulbrich, A., Coon, J.J., et al. (2014). Formic-acid-induced depolymerization of oxidized lignin to aromatics. Nature ***515***(7526): 249–252. https://doi.org/10.1038/nature13867.
61. Hahladakis, J.N., Velis, C.A., Weber, R., et al. (2018). An overview of chemical additives present in plastics: migration, release, fate and environmental impact during their use, disposal and recycling. J. Hazard Mater. ***344***: 179–199. https://doi.org/10.1016/j.jhazmat.2017.10.014.
62. Ilton, E.S., Post, J.E., Heaney, P.J., et al. (2016). XPS determination of Mn oxidation states in Mn (hydr)oxides. Appl. Surf. Sci. ***366***: 475–485. https://doi.org/10.1016/j.apsusc.2015.12.159.
63. Biesinger, M.C., Payne, B.P., Grosvenor, A.P., et al. (2011). Resolving surface chemical states in XPS analysis of first row transition metals, oxides and hydroxides: Cr, Mn, Fe, Co and Ni. Appl. Surf. Sci. ***257***(7): 2717–2730. https://doi.org/10.1016/j.apsusc.2010.10.051.
64. Xu, T., Li, G., and Zhao, L. (2018). Ni-Co-S/$Co(OH)_2$ nanocomposite for high energy density all-solid-state asymmetric supercapacitors. Chem. Eng. J. ***336***: 602–611. https://doi.org/10.1016/j.cej.2017.12.065.
65. Reed, G.H., Leigh, J.S., Jr., et al. (1971). Electron paramagnetic relaxation and EPR line shapes of manganous ion complexes in aqueous solutions. Frequency and ligand dependence. J. Chem. Phys. ***55***(7): 3311–3316. https://doi.org/10.1063/1.1676582.
66. Partenheimer, W. (2001). The structure of metal/bromide catalysts in acetic acid/water mixtures and its significance in autoxidation. J. Mol. Catal. A-Chem. ***174***(1): 29–33. https://doi.org/10.1016/S1381-1169(01)00169-8.
67. Partenheimer, W. (1995). Methodology and scope of metal/bromide autoxidation of hydrocarbons. Catal. Today ***23***(2): 69–158. https://doi.org/10.1016/0920-5861(94)00138-R.
68. Maity, A., Hyun, S.-M., and Powers, D.C. (2018). Oxidase catalysis via aerobically generated hypervalent iodine intermediates. Nat. Chem. ***10***(2): 200–204. https://doi.org/10.1038/nchem.2873.
69. Larkin, D.R. (1990). The role of catalysts in the air oxidation of aliphatic aldehydes. J. Org. Chem. ***55***(5): 1563–1568. https://doi.org/10.1021/jo00292a035.

ACKNOWLEDGMENTS

We acknowledge the NSFC (Nos. 22293014, 22131002, 22161142019), the National Key R&D Program of China (No. 2021YFA1501700), and the New Cornerstone Science Foundation through the XPLORER PRIZE for financial support. We would also like to thank our colleagues Prof. Jian Pei, Prof. Rong Zhu, and Prof. Aiwen Lei for sharing their instruments and helpful suggestions; Dr. Zhenjin Liang and Ms. Qinqin Wei for their helpful discussions; and Mr. Zhenpeng Wang for his help in the analytical testing.

AUTHOR CONTRIBUTIONS

N.J. and B.Z. conceived the research idea. N.J. directed the research. B.Z., H.T., and N.J. wrote the paper. B.Z., X.Z., Z.Y., H.S., and Y.Z. performed the experiments. Y.F. and J.D. supervised the Techno-Economic Analysis (TEA) and Life Cycle Assessment (LCA) calculations. J.Y. performed the TEA and LCA calculations. B.Z., H.T, J.W., X.Z., L.C., D.Y., and Z.H. discussed the results.

DECLARATION OF INTERESTS

The authors declare no competing interests.

SUPPLEMENTAL INFORMATION

It can be found online at https://doi.org/10.1016/j.xinn.2024.100586.

LEAD CONTACT WEBSITE

http://sklnbd.bjmu.edu.cn/team/jiaoning/eng/